

1 Research paper

2 **The importance of variation in offspring body size for stability in cannibalistic populations**

3 **ABSTRACT**

4 Animals exhibit remarkable intraspecific variation in phenotypic traits such as body size.

5 Understanding how such trait variation affects population and ecosystem dynamics is critically
6 important, because future environmental change and human impacts are expected to alter

7 phenotypic trait distributions. In species with seasonal reproduction, offspring size variation

8 within cohorts is ubiquitous, yet we know little about its implications for population stability. In

9 addition, long-term monitoring data indicate that changes in offspring size variation occur at

10 ecologically relevant time scales. Here, we study the consequences of changing offspring size

11 variation by developing and analysing an integral projection model (IPM). Our model accounts

12 for size-dependent cannibalism as well as additional density regulation occurring during the first

13 year. The model is parameterized using literature values and long-term monitoring data for pike

14 (*Esox lucius*), a common fish predator in temperate freshwater ecosystems, but the general model

15 structure applies to a wide range of size-structured organisms. Our analyses demonstrate that a

16 wide size distribution of offspring promotes stable dynamics, whereas narrow distributions can

17 be destabilizing because cannibalism increases the annual variation in mean offspring mortality.

18 Our results indicate that the stabilizing effect of offspring size variation is likely an important

19 property of size-structured organisms with seasonal reproduction and cannibalistic behaviour.

20 This work highlights the importance of intracohort trait variation and describes how variation in

21 body size can shape the dynamics of animal populations.

22 **Keywords:** integral projection model, intraspecific interactions, trait variation

23 INTRODUCTION

24 Most animal populations exhibit large amounts of variation in phenotypic traits, because
25 individuals differ in their genetic makeup, behavioural strategies, and experienced environmental
26 conditions (Ebenman and Persson 1988; Bolnick et al. 2003). The role of intraspecific trait
27 variation in shaping ecological and evolutionary processes at the species and community levels
28 has recently received increased attention (Bolnick et al. 2011; Dall et al. 2012; de Roos and
29 Persson 2013; Vindenes and Langanen 2015; Hart et al. 2016). **While the effects of individual
30 variation (e.g. variation in body size, resource partitioning, or variation arising from ontogenetic
31 development) on the stability of populations have previously been investigated (Łomnicki 1988;
32 DeAngelis et al. 1993; Bjørnstad and Hansen 1994; Claessen et al. 2000; van Kooten et al. 2010),
33 we still have limited understanding of the population dynamical consequences of initial trait
34 variation within cohorts, i.e. groups of similar-aged individuals (but see van Kooten et al. 2004).**

35 Intracohort variation in offspring body size is ubiquitous in populations that exhibit discrete
36 reproductive periods, i.e. most species in seasonal environments (e.g., Uchmanski 1985; Einum
37 and Fleming 2002; Pfister and Stevens 2002). Moreover, long-term ecological monitoring data
38 suggest that significant changes in offspring size distributions occur over ecologically relevant
39 time periods. For instance, empirical data suggest decreasing variation in offspring size for well-
40 studied freshwater (e.g. pike (*Esox lucius*): Supplementary Material, Appendix 1) and marine
41 (e.g. Atlantic cod (*Gadus morhua*): Olsen et al. 2009) fish populations. Understanding how trait
42 variation affects the dynamics of populations and ecosystem functioning is a fundamental
43 challenge in ecology that is becoming increasingly important due to intensified human impacts
44 and altered environmental conditions that may cause widespread changes in phenotypic trait
45 distributions (Moran et al. 2015).

46 Various ecological processes contribute to variation in offspring size. Potential mechanisms
47 include (i) genetic variation, (ii) social structure, e.g. resource monopolization, (iii) maternal
48 effects, (iv) small-scale heterogeneity in environmental conditions, (v) variation in the time of
49 hatching or emergence, and (vi) random events such as disease outbreaks (Johnston and Leggett
50 2002; Pfister and Stevens 2002; Huss et al. 2007; Peacor et al. 2007; Rasmussen and Rudolf
51 2015). Producing offspring of variable size may also constitute a form of bet-hedging, i.e. an
52 adaptation that buffers reproductive success against unpredictable environments (Philippi and
53 Seger 1989; Einum and Fleming 2002; Marshall et al. 2008). Increased environmental variability
54 due to climate change may indeed favour differential investment and consequently higher size
55 variation among offspring. Prolonged or contracted reproductive periods due to climate-induced
56 phenological change are also expected to affect offspring size distributions, which depend on the
57 length of the reproductive season (Keast and Eadie 1984; Rasmussen and Rudolf 2015). Shorter
58 reproductive periods may be caused by truncated parental size distributions due to size-selective
59 removal (Wright and Trippel 2009). While many processes that contribute to variation in
60 offspring body size have been identified, its consequences for the dynamics of populations have
61 received less attention. Variation in offspring size could be an important driver of population
62 dynamics, because it affects the ecological interactions among individuals such as intraspecific
63 predation (cannibalism) and competition which depend on body size.

64 Understanding the broader implications of changes in size variation for population stability
65 requires a framework that accounts for continuous size-structure and incorporates size-dependent
66 interactions. Integral projection models (IPMs) provide such a framework, by linking individual-
67 level trait-dependent demographic processes and ecological interactions to population-level
68 dynamics (Easterling et al. 2000; Ellner et al. 2016). Other models such as physiologically

69 structured population models (de Roos et al. 1992) meet these requirements and have been used
70 to study size-based interactions within populations, including cannibalism (Claessen et al. 2000).
71 Integral projection models are discrete time models that belong to the same class as matrix
72 models, and therefore share their analytical advantages (Ellner and Rees, 2006). The dynamics of
73 the trait structure are determined by the main vital rate functions that describe how survival,
74 growth, reproduction, and the initial state distribution of offspring depend on the underlying state
75 variable(s). These functional relationships can be determined from data using regression methods.
76 IPMs provide a powerful data-driven framework for studying the ecological (and evolutionary)
77 dynamics of populations (Coulson 2012; Vindenes and Langanen 2015, Ellner et al. 2016). In
78 recent years several extensions have been made to increase the range of applications of IPMs,
79 including the effects of climate change (Simmonds and Coulson 2014, Vindenes et al. 2014;
80 2016), yet the majority of applications so far ignore trait-based interactions among individuals
81 (but see Bassar et al. 2016). The incorporation of such interactions thus represents a great
82 potential for new applications of the framework both for theoretical and empirical investigations.
83 A few IPM applications have incorporated size-based competition (Bassar et al. 2016), but
84 intraspecific predation, i.e. cannibalism, has to our knowledge not been studied within this
85 framework.

86 Cannibalism and competition are complex intraspecific interactions that affect processes such as
87 growth and survival. Both types of interaction can alter the size distribution within cohorts (Huss
88 et al. 2007, 2008, 2010), and their effects on population dynamics may depend on hatchling size
89 (van Kooten et al. 2010). Cannibalism affects individual growth and size-dependent survival
90 because cannibals and victims typically differ in body size yet may compete (at least in part) for
91 shared resources. In particular, cannibalism often has a large impact on the survival of victims

92 though size-dependent predation. Cannibalistic behaviour is a common phenomenon found in all
93 major animal taxa in aquatic and terrestrial systems (e.g. protozoa, arthropods, gastropods,
94 sharks, bony fishes, amphibians, reptiles, birds, and mammals), and is known to constitute a
95 major cause of mortality in many species, especially among early life-stages (Fox 1975; Polis
96 1981). Cannibalism is an inherently size-dependent interaction that has been widely studied in the
97 theoretical literature and has been shown to affect population and community dynamics (Briggs
98 et al. 2000; Persson et al. 2003; Claessen et al. 2004; Rudolf et al. 2007; Huss et al. 2010).
99 However, knowledge of how population stability in cannibalistic species depends on the size
100 variation among offspring is lacking. We therefore developed an IPM that incorporates size-
101 dependent cannibalism to study how size variance in offspring (here: 1-year-old fish) affects
102 population dynamics and demography. We parameterized the model for pike, a freshwater top-
103 predator known to show cannibalistic behaviour. However, the model can easily be adapted to
104 other size-structured organisms with other kinds of trait-based interactions (e.g. competition), and
105 we demonstrate that our main result, the stabilizing effect of offspring size variation, is valid
106 across a wide range of conditions.

107 **METHODS**

108 **Model description**

109 **Baseline IPM**

110 For simplicity, we first describe a basic IPM of a population that is structured according to a
111 continuous state variable x , here size (length in cm). In the next section we extend the model to a
112 density-dependent model including size-dependent cannibalism. We consider a female-based
113 model with annual time steps. The size distribution of individuals at time t is $\mathbf{n}_t = n_t(x)$, so that

114 the total population size is $N_t = \int_0^\infty n_t(x)dx$. Without density dependence, the change in the size
 115 distribution from one year to the next is given by

$$116 \quad n_{t+1}(x') = \int_0^\infty [s(x)g(x';x) + b(x)f(x';x)]n_t(x)dx,$$

117 where for an individual of current size x , $s(x)$ is the annual survival probability, $g(x';x)$
 118 represents growth (the distribution of next year's size x'), $b(x)$ is the number of offspring
 119 produced that survive until next year's population (pre-reproductive) census, and $f(x';x)$ is the
 120 distribution of offspring size x' as they enter the population next year, potentially depending on
 121 the parent's size x . Together, these four vital rates determine the projection kernel, which is
 122 equivalent to the projection matrix in matrix models (Easterling et al., 2000), and each vital rate
 123 can be decomposed further into underlying processes. We have extended the baseline IPM in two
 124 main ways, to incorporate i) size-dependent cannibalism, which can potentially affect any vital
 125 rate, and ii) additional density-dependent feedbacks occurring in the first year of life (typical for
 126 fish life histories), regulating survival and growth during the first year. We describe these
 127 extensions below where each vital rate is defined in more detail. The sequence of annual life-
 128 history events is illustrated in Figure 1. In the following notation, density- and size-dependent
 129 functions have a subscript t .

130 **Cannibalism kernel**

131 Size-dependent cannibalism has previously been studied with continuous-time models, and we
 132 will largely follow the general processes and terminology defined by Claessen et al. (2000)
 133 although simplified and adapted to a discrete time IPM. In the following, y denotes cannibal size,
 134 while x refers to victims (note that the same individual can be both a cannibal, preying on smaller
 135 individuals, and a victim if preyed upon by larger ones). We define a cannibalism kernel $C_{cn}(x,y)$

136 that describes the distribution of potential prey sizes for each cannibal size y , i.e. the likelihood
 137 that an individual of size x is in the diet range of the cannibal ($\int_0^\infty C_{cn}(x,y)dx = 1$). This kernel
 138 can be defined in several ways, depending on the life history and behaviour of the organism. We
 139 assume that the victim to cannibal length ratio x/y follows a lognormal distribution $LN(\frac{x}{y}, \mu_{cn}, \sigma_{cn}$
 140) with scale parameter σ_{cn} and location parameter μ_{cn} . The cannibalism kernel is given by the
 141 normalized function $C_{cn}(x,y) = LN(\frac{x}{y}, \mu_{cn}, \sigma_{cn})/y$ (where $\int_0^\infty LN(\frac{x}{y}, \mu_{cn}, \sigma_{cn})dx = y$). This implies
 142 that the range of potential victim sizes (cannibalism window) increases with cannibal size (Figure
 143 2a). Claessen et al. (2000) used a tent function with a similarly increasing cannibalism window
 144 with size. This kernel can be incorporated in the definition of any vital rate function to capture
 145 effects of cannibalism. Here, we assume that cannibalism mainly affects survival of the victims
 146 and that for the modelled population cannibals have alternative prey whenever smaller
 147 conspecifics are not available, i.e. growth is independent of any single food source. **This**
 148 **assumption applies to opportunistic predators that feed on several species of alternative prey,**
 149 **such as pike in Windermere, UK (Winfield et al. 2012).**

150 ***Survival including size-dependent cannibalism***

151 In addition to the cannibalism kernel defined above, the effects of cannibalism depend on the
 152 cannibal attack rate (Claessen et al., 2000). For a cannibal of size y , the relative attack rate on
 153 victims of size x is given by $\beta_{cn}y^{\alpha_{cn}}C_{cn}(x,y)$, where the parameter β_{cn} defines the overall
 154 cannibalism intensity, and $\alpha_{cn}(\alpha_{cn} < 1)$ scales this intensity to cannibal size y . Thus, the annual
 155 encounter rate of a cannibal with potential victims is given by

$$156 \quad \gamma_{cn,t}(y) = \int_0^\infty \beta_{cn}y^{\alpha_{cn}} C_{cn}(x,y) n_t(x)dx.$$

157 The overall mortality risk of an individual of size x due to cannibalism also depends on the size
 158 distribution of cannibals and the kind of functional response shown by the cannibals, given by

$$159 \quad \omega_{cn,t}(x) = \int_0^{\infty} \frac{\beta_{cn} y^{\alpha_{cn}} C_{cn}(x,y) n_t(y)}{1 + \delta_{cn} \gamma_{cn,t}(y)} dy.$$

160 Here, the parameter δ_{cn} determines the functional response of the cannibal, where $\delta_{cn} = 0$ yields
 161 a type I response (Holling 1959), i.e. victim population density does not restrict cannibals, and
 162 $\delta_{cn} > 0$ yields a type II response, i.e. cannibalism mortality approaches a maximum at high
 163 victim densities. If cannibalism is the only source of mortality, the survival probability of a size x
 164 victim is $s_{cn,t}(x) = \exp(-\omega_{cn,t}(x))$. However, other sources of mortality are also likely to be
 165 present, such as predation from other species, diseases, and starvation. Here we include another
 166 term capturing this background mortality, and for the pike model we assume it is density
 167 independent but non-linear so that small and very large (old) individuals have a higher

168 background mortality than intermediate sized ones (figure 2b): $s_b(x) = \frac{2s_{b0}}{1 + e^{\beta_{sb}(x - \alpha_{sb})^2}}$. The initial

169 increase in background survival with size is assumed to reflect a reduction in starvation
 170 probability and interspecific predation, while the decrease for very large individuals reflects
 171 fishing mortality and senescence related to increasing risk of infection with parasites and other
 172 diseases (Haugen et al. 2007). Including both sources of mortality, the survival function becomes:

$$173 \quad s_t(x) = s_b(x) s_{cn,t}(x)$$

174 **Growth**

175 Conditional on the current length x , next year's length x' follows a lognormal distribution g
 176 $(x';x)$, with a mean $\mu_g(x)$ according to a von Bertalanffy growth function, and a variance $\sigma_g^2(x)$
 177 in the growth increments that declines exponentially with size, i.e. $\sigma_g^2(x) = \tau_g^2 e^{-2\nu_g x}$. This

178 implies that the unconditional variance in size at age increases early in life up to age-3 and
 179 thereafter decreases. We assume constant food availability and growth, though food-dependent
 180 growth is accounted for in the extended model that includes effects of competition (Appendix 3).
 181 Mean length next year (on log scale), given current length x , is $\mu_g(x) = \ln [KL_\infty + (1 - K)x]$.
 182 Here, K is the von Bertalanffy growth rate, and L_∞ is asymptotic length. We require $\mu_g(x) > x$,
 183 and otherwise we set $\mu_g(x) = x$, i.e. the expected growth rate cannot be negative (Figure 2c).

184 After growth and survival, population size without offspring is given by $n_t^*(x') = \int_0^\infty n_t(x) s_t(x)$
 185 $g(x';x) dx$.

186 ***Reproduction and first year processes***

187 Let M_t denote the total number of eggs the population can produce in year t . Multiple density-
 188 dependent processes may contribute to reduce this number until the resulting offspring are
 189 counted at age 1, including parental competition for reproduction sites, as well as competition,
 190 predation, and disease affecting individuals during their first year of life. To capture all of these
 191 processes we included a general model for density dependence for egg production and during the
 192 first year after eggs are produced. Letting $f_t(x')$ denote the size-distribution of offspring at age 1
 193 (described below), the total number of offspring after this density regulation is given by

$$194 \quad R_t(x') = f_t(x') \frac{\alpha_R M_t}{1 + \beta_R M_t},$$

195 where α_R is the slope at origin (i.e. number of offspring resulting from very low egg numbers),
 196 and β_R is a capacity parameter such that α_R/β_R is the maximum number of offspring (Figure 2d).
 197 Before entering next year's population, the offspring number can be further reduced by size-
 198 dependent cannibalism by the rest of the population (Figure 1). This intercohort cannibalism
 199 during the first year is assumed to occur after growth (as determined by $f_t(x')$), but before the

200 next census, thus the population of potential cannibals of the offspring is given by $n_t^*(x')$
 201 (Figure 1). This model simplification is reasonable when hatchlings are too small to be
 202 effectively predated by older conspecifics, or when they are spatially segregated from later life
 203 stages (Pereira et al. 2017), for instance due to association of young fish with vegetation, as
 204 found in pike (Bry 1996). The number of offspring that enter the next census is then given by O_t
 205 $(x') = R_t(x') s_{cn,t}^*(x')$, where $s_{cn,t}^*(x')$ represents the survival of offspring after cannibalism by
 206 $n_t^*(x')$, and next year's population distribution is $n_{t+1}(x') = n_t^*(x') + O_t(x')$.

207 Looking into each of the components of $R_t(x')$ in more detail, the total number of eggs produced
 208 is given by $M_t = 0.5 \int_0^\infty n_t(x) m(x) p_m(x) dx$, where $m(x)$ is the fecundity (mean number of
 209 eggs) of a female of length x , and $p_m(x)$ is the probability of being mature at size x (the factor
 210 0.5 reflects the assumption of a 1:1 sex ratio). Probability of maturity $p_m(x)$ is assumed to follow
 211 a sigmoid function (Figure 2e) with $p_m(x) = \frac{1}{1 + e^{-\sigma_p(x - \mu_p)}}$, where μ_p is mean size at maturation
 212 and σ_p determines the slope on the logit scale. Fecundity $m(x)$ is assumed to follow a power
 213 function (Figure 2e) $m(x) = \alpha_m x^{\beta_m}$, where α_m is a constant and β_m is a size-scaling exponent.
 214 The length distribution of offspring $f_t(x')$ is assumed to be independent of parental length, and to
 215 follow a lognormal distribution with a constant variance on linear scale σ_{L1}^2 (a key parameter to
 216 be varied in the model analysis) and a mean $\mu_{L1,t}$. This parameter depends on the total egg
 217 number: $\ln \mu_{L1,t} = \beta_{0L1} - \beta_{ML1} \ln M_t$ (Vindenes et al. 2016), and thus captures effects of density
 218 dependence on growth during the first year (see also Appendix 4).

219 ***Model analysis: Changing the variance in offspring size distribution***

220 We used this model to analyse population dynamics over a large range of variances in offspring
221 size σ_{L1}^2 (see Figure 2f). The effect on population stability was investigated using bifurcation
222 analysis, which was performed by running the IPM for each discrete variance value to record the
223 population size distribution projected over 1000 time steps. Population size for the last 100 time
224 steps was plotted against the variance in offspring length to assess population stability (a
225 population at equilibrium is characterized by a single population size, whereas unstable
226 dynamics, i.e. with cyclic or chaotic behaviour, are represented by multiple population sizes).

227 To account for uncertainty in parameter values, we explored a broad range of values for other key
228 parameters in the model as part of our sensitivity analysis, including mean offspring size (μ_{L1}) the
229 strength of cannibalism (β_{cn}), and growth variation later in life (τ_g). The entire analysis was
230 repeated for a model including size-dependent competition in addition to cannibalism, to confirm
231 the robustness of our main conclusion (Supplementary Material, Appendix 3). All analyses were
232 performed in R (v.3.3.2, R Core Team, 2016).

233 **Model parameterization**

234 As detailed below, model parameters were based on literature values and data from a long-term
235 monitoring program for pike in the lake of Windermere, UK (Le Cren 2001; Vindenes et al.
236 2014; Winfield et al. 2013a, b, 2015). This dataset contains measurements of length, age, sex, and
237 body mass of individual pike collected over a period of 50 years (1946-1995), including
238 **estimates of length-at-age that were back-calculated using opercular bones**, as well as estimates
239 of the number of eggs per female. Associated diet data show that pike in Windermere predate a
240 range of species in addition to conspecifics, including Arctic charr (*Salvelinus alpinus*), brown
241 trout (*Salmo trutta*), perch (*Perca fluviatilis*), and roach (*Rutilus rutilus*) (Winfield et al. 2012).

242 **Survival:** Parameters of the background survival function were set to $\alpha_{sb} = 80$, $\beta_{sb} = -0.0005$, and
243 $s_{b0} = 1.7$ (Figure 2b). The location and scale parameters of the cannibalism kernel were set to
244 $\mu_{cn} = -1.5$ and $\sigma_{cn} = 0.3$ (minimum cannibal size was 5 cm), such that the relative sizes of
245 preferred prey in all size classes agreed with literature values (Mittelbach and Persson 1998;
246 Persson et al. 2006; Figure 2a). Reported lower and upper limits for the victim-to-cannibal size
247 ratio in pike are 0.03 and 0.55 (Persson, Bertolo & de Roos 2006). The scaling parameter of the
248 maximum cannibalistic attack rate was set to $\alpha_{cn} = 0.6$ (Claessen et al. 2000) and we used $\delta_{cn} = 0.1$
249 for a type II functional response, the most frequently observed functional form (Begon et al. 2006).
250 Cannibalistic voracity was set to $\beta_{cn} = 0.01$ to reflect reasonable mortality rates. This parameter
251 could not be estimated from our data or taken from the literature and was thus varied as part of
252 the model analysis.

253 **Growth:** Von Bertalanffy growth parameters $K = 0.21$ and $L_{\infty} = 109$ cm were estimated from data
254 on Windermere pike (Figure 2c). The variance in growth, which declines exponentially with size
255 according to the empirical data (Vindenes et al. 2014), was modelled using $\nu_g = -0.015$ and $\tau_g = 5$.
256 We considered a size range of 5-130 cm. For the numerical calculations, we used 500 mesh
257 points for the continuous state variable, i.e. 500 size classes with a size difference of ~ 0.25 cm.

258 **Reproduction:** The maturation parameters were set to $\mu_p = 41.5$ and $\sigma_p = 0.5$ to match data from
259 Windermere where female pike first spawn at ~ 31 -50 cm (Figure 2e Frost & Kipling 1967). The
260 size-fecundity relationship was also estimated from empirical data from Windermere. Estimates
261 of the intercept and slope of the log-log relationship between the number of eggs and body length
262 were $\alpha_m = 0.095$ and $\beta_m = 3.3$ (Figure 2e). **In the absence of robust empirical data**, it is assumed that
263 newly hatched offspring experience density regulation prior to the first census. The parameters of the
264 asymptotic relationship were set to $\alpha_R = 4 \cdot 10^{-4}$ and $\beta_R = 1 \cdot 10^{-8}$ (Figure 2d). Finally, the offspring

265 size distribution was assumed to follow a lognormal distribution (in line with the data), where
266 mean length depends on the total number of eggs according to an exponential decrease with
267 parameters $\beta_{OL1} = 3.85$ and $\beta_{ML1} = 0.04$.

268 **RESULTS**

269 Changes in offspring size variance have strong and consistent effects on population stability
270 (Figure 3). Population dynamics are stable at wide offspring size distributions, but unstable at
271 narrow size distributions (see Figure 2f for reference). The unstable dynamics at low variances
272 alternate between cyclic fluctuations, as reflected by distinct recurring population densities, and
273 irregular fluctuations in population size (Figure 3). The range of population densities decreases
274 with increasing size variance until the threshold is reached and the dynamics become stable. At
275 low offspring size variance, the population exhibits oscillations that are not dampened over time,
276 and a stable size distribution is not reached (Figure 4a). Instead, the density of offspring that enter
277 the population and consequently the densities of older cohorts both fluctuate (Figure 4c), due to
278 strongly varying probabilities of surviving cannibalism (Figure 4e). In contrast, with high
279 variance in offspring size the population reaches an equilibrium size (Figure 4b). A stable size
280 distribution is reached showing a size structure with distinct age-cohorts (Figure 4d). In the stable
281 case, survival probability of small individuals is constant and rather low due to high cannibalism,
282 whereas survival probability of large individuals is relatively high and mostly determined by
283 density-independent mortality (Figure 4f; offspring survival rates over time are shown in the
284 Supplementary Material, Appendix 2).

285 By including the effects of intraspecific competition for resources on individual growth and
286 survival into our model, we further show that the occurrence of the stability-instability pattern
287 across the range of offspring size variance does not critically depend on the strength of

288 intraspecific competition, at least when cannibalism is sufficiently strong and competition is
289 assumed to be most intense among individuals of similar body size (Supplementary Material,
290 Appendix 3). Additional sensitivity tests showed that the destabilization at low values of the
291 offspring size variance occurs for a wide range of cannibalism interaction strengths. In the
292 sensitivity analysis, cannibalism and competition intensity were varied widely to cover a broad
293 range of ecologically relevant interaction strengths, thus representing large variation in growth
294 rates and survival probabilities. Importantly, the stability-instability transition disappears at (i)
295 small mean offspring sizes, (ii) large victim-to-cannibal size ratios, or (iii) high variances of
296 the cannibalism kernel, which results in stable population dynamics irrespective of the offspring
297 size variance (Supplementary Material, Appendix 4). **Furthermore, the stability-instability**
298 **transition is shifted to lower variance values as variation in individual growth increases.**
299 Therefore, other aspects of the ecological interaction between individuals also matter for the
300 population dynamical response to changes in the variance in offspring size. Overall, our
301 sensitivity analysis showed that the population dynamics are either stable throughout the range of
302 offspring size variances or exhibit a transition to unstable dynamics at low size variance, as
303 presented in Figure 3.

304 **DISCUSSION**

305 We have developed an integral projection model including size-dependent cannibalism as well as
306 additional density regulation at the offspring stage. The main conclusion from our analysis is that
307 the amount of individual variation in offspring size affects population stability. In our model the
308 population dynamics become increasingly unstable as the size variation decreases, and become
309 more stable as the variation in offspring body size increases. Earlier work suggested that trait
310 variation in general affects population growth and stability, and that stabilizing or destabilizing

311 effects can be predicted from unstructured population models where the trait distribution depends
312 only on population density (Bjørnstad and Hansen 1994). We used a more complex model with
313 continuous size-structure and overlapping generations, which suggests that a stabilizing effect of
314 variation in offspring body size may be generalized to size-structured organisms that are
315 characterized by seasonal reproduction and cannibalistic behaviour. Similar life-histories may be
316 particularly wide-spread among fish species at mid or high latitudes (Pereira et al. 2017).

317 The shift from stable to unstable dynamics as offspring size variance decreases is driven by a
318 range of complex size-dependent processes. One of the key processes affecting this transition is
319 offspring mortality, which strongly depends on intercohort cannibalism and in turn has a strong
320 influence on the population dynamics. The offspring size distribution sets the starting point for
321 subsequent growth and therefore influences the entire size distribution. A large offspring size
322 variance leads to broad cohort peaks in the population size distribution, while a low size variance
323 leads to pronounced cohort peaks. A size distribution without strong peaks implies little
324 interannual variation in the risk of cannibalism, where offspring mortality from intercohort
325 predation can be high but it is stable, thus preventing the occurrence of strong or weak cohorts.
326 As the offspring size distribution is narrowed, the cohort peaks in the population size distribution
327 become more pronounced such that more individuals of a given cohort escape cannibalism if they
328 are outside the victim size range, or are cannibalized if they are within the victim size range.
329 These individuals subsequently contribute to a higher (or lower) density of cannibals, thus
330 increasing (or decreasing) the mortality among new victims. Such density-dependent feedbacks
331 in intercohort cannibalism give rise to fluctuations in annual offspring mortality and population
332 size. As offspring size variance is further reduced, the fluctuations increase (Figure 3), such that
333 at extremely low offspring size variance most of the offspring cohort either escapes cannibalism

334 (when the number of potential cannibals is low), or is cannibalized (when preyed upon by a
335 preceding cohort that was not heavily cannibalized). Hence, mean offspring mortality is high
336 whenever the offspring size distribution matches the cannibalism window of preceding cohorts
337 (Figure 4). The population dynamics are therefore characterized by the dominance of strong
338 cohorts. This feedback, which prevents stabilization of the population dynamics, results from the
339 interplay between the size distributions of the interacting cohorts and intercohort predation
340 (cannibalism and background survival rates are shown in Figure A2, Supplementary Material).
341 Intercohort cannibalism on offspring thus plays a crucial role in causing unstable dynamics. The
342 exact quantitative pattern of where the shift occurs, or whether it occurs at all, is modified by
343 other processes in the model, such as the growth model (mean and variance), the strength of
344 cannibalism, and the cannibalism window as determined by the cannibalism kernel, but the
345 qualitative pattern of increased stability at higher offspring size variance remains the same across
346 all our tested conditions (see Supplementary Material, Appendix 4).

347 Previous studies have largely found destabilizing effects of cannibalism on population dynamics,
348 yet stabilizing effects have also been reported (Cushing 1991; Hastings and Costantino 1991;
349 Briggs et al. 2000; Claessen et al. 2000). Importantly, when cannibals are able to feed efficiently
350 on new recruits, cannibal-driven cycles can occur due to the high mortality induced among
351 victims (Claessen et al. 2002; Persson et al. 2006). Whether cannibals can efficiently feed on
352 recruits also depends on the cannibalism window and initial hatchling size (Persson et al. 2004;
353 van Kooten et al. 2010). Here we show that this is more likely to occur when the offspring size
354 variation is low compared to the cannibalism size window. Similarly, adult-driven cohort cycles
355 can occur when large individuals are competitively superior over small ones (Briggs et al. 2000;
356 de Roos and Persson 2013). Both competitive superiority and cannibalism by larger conspecifics

357 represent strongly asymmetric intraspecific interactions. In contrast, when small individuals are
358 competitively superior, they may outcompete their larger conspecifics and induce juvenile-driven
359 cycles. Whether or not increased offspring variation may lead to unstable dynamics in such cases
360 remains to be explored.

361 The long-term monitoring data from Windermere suggest that the variance in body size of 1-
362 year-old pike has declined over a time period of 50 years (Supplementary Material, Appendix 1).
363 Our model results indicate that a population experiencing such continuous declines in offspring
364 size variance may be approaching increasingly unstable dynamics. While environmental changes
365 have profoundly altered this freshwater ecosystem over the past few decades, including increased
366 water temperatures (Ohlberger et al. 2013), fundamental changes in the fish community
367 (Winfield et al. 2012), and shifts in the phenology of the fish and plankton communities
368 (Thackeray et al. 2013), the causes of the reduction in size variance in Windermere pike are not
369 known and merit further investigation. Our model assumes constant size variance to study the
370 consequences of such variation; when underlying mechanisms of the size variation are identified,
371 these could be incorporated into the model. The population does not currently show signs of
372 instability. While the trend in offspring size variance is decreasing, size variance has generally
373 been large, and there is considerable variation in size variance among years, both of which seem
374 to prevent unstable dynamics. Additionally, other factors not accounted for in our model such as
375 environmental stochasticity in survival might have a stabilizing effect. It is worth noting that the
376 range in offspring size variance analysed in this study, which is equivalent to a coefficient of
377 variation of up to ~20%, encompasses size variances reported for other species. For freshwater
378 and marine fishes, the CV in size of egg and larval stages has generally been found to range from
379 3%-12% (for comparisons of multiple species see: Hutchings 1997; Einum and Fleming 2002),

380 whereas size variation among juveniles is typically larger, with reported values of 8%-23%
381 (several fish species: van Densen et al. 1996; Nordwall et al. 2001). Most of the species examined
382 in those studies are characterized by seasonal reproduction and cannibalistic behaviour.

383 The importance of phenotypic trait variation has long been recognized in evolutionary ecology,
384 because variation in heritable traits provides the basis for natural selection. Changes in trait
385 distributions due to altered ecological processes can facilitate adaptive evolution if reproductive
386 fitness is increased under novel ecological conditions. One example would be increased climatic
387 variability favouring differential maternal investment and thus higher variation in offspring body
388 size. Similar changes could arise in response to human impacts such as harvesting. The resulting
389 feedbacks between trait evolution and ecological processes are important to consider when
390 evaluating potential consequences of altered trait distributions. Such eco-evolutionary feedback
391 dynamics related to individual trait variation have recently received increasing attention (Bolnick
392 et al. 2011; Vindenes & Langangen 2015). The model presented here provides a starting point for
393 future investigations of eco-evolutionary dynamics, for instance by letting the offspring size
394 distribution depend on maternal size.

395 This work extends the demographic modelling framework of IPMs to include cannibalism, a
396 widespread and inherently size-dependent intraspecific interaction. Our main result demonstrates
397 how individual size variation within cohorts can profoundly affect the dynamics of animal
398 populations, and that increased variation in offspring body size stabilizes population dynamics
399 under a wide range of conditions. In a broader context, our work adds to the growing evidence of
400 the importance of early-life processes (e.g., maternal effects and cohort effects) for individuals
401 and populations. Future developments of our modelling framework include considering species
402 interactions and investigating the dynamical consequences of stochastic variation in offspring

403 size distributions. Empirical studies should further investigate the potential mechanisms leading
404 to changes in size variation and evaluate the empirical evidence for associated shifts in
405 population dynamics.

406 **DECLARATIONS**

407 *Acknowledgements:* We gratefully acknowledge the many researchers at the Centre for Ecology
408 & Hydrology (Lancaster, UK) and at the Freshwater Biological Association (Ambleside, UK)
409 who have undertaken the field and laboratory work for the long-term scientific monitoring of
410 Windermere pike.

411 **REFERENCES**

- 412 Bassar, R.D. et al. 2016. The effects of asymmetric competition on the life history of Trinidadian
413 guppies. – *Ecol. Lett.* 19: 268–278.
- 414 Begon, M. et al. 2006. *Ecology: from individuals to ecosystems*. – Blackwell Publishing, Oxford.
- 415 Bjørnstad, O.N. and Hansen, T. 1994. Individual variation and population dynamics. – *Oikos* 69:
416 167–171.
- 417 Bolnick, D.I. et al. 2011. Why intraspecific trait variation matters in community ecology. –
418 *Trends Ecol. Evol.* 26: 183–192.
- 419 Bolnick, D.I. et al. 2003. The ecology of individuals: incidence and implications of individual
420 specialization. – *Am. Nat.* 161: 1–28.
- 421 Briggs, C. J. et al. 2000. What causes generation cycles in populations of stored-product moths? –
422 *J. Anim. Ecol.* 69: 352–366.
- 423 Bry, C. 1996. Role of vegetation in the life cycle of pike. – In J. F. Craig (ed.) *Pike: Biology and*
424 *Exploitation*. Chapman & Hall, London, pp. 45-67.

- 425 Claessen, D. et al. 2000. Dwarfs and giants: cannibalism and competition in size-structured
426 populations. *Am. Nat.* 155: 219–237.
- 427 Claessen, D. et al. 2004. Population dynamic theory of size-dependent cannibalism. – *Proc. Roy.*
428 *Soc. B* 271: 333–340.
- 429 Claessen, D. et al. 2002. The impact of size-dependent predation on population dynamics and
430 individual life history. – *Ecology* 83: 1660–1675.
- 431 Coulson, T. 2012. Integral projections models, their construction and use in posing hypotheses in
432 ecology. – *Oikos* 121: 1337–1350.
- 433 Cushing, J.M. 1991. A simple model of cannibalism. *Math. Biosci.* 107: 47–71.
- 434 Dall, S.R.X. et al. 2012. An evolutionary ecology of individual differences. – *Ecol. Lett.* 15:
435 1189–1198.
- 436 de Roos, A et al. 1992. Studying the dynamics of structured population models: a versatile
437 technique and its application to *Daphnia*. – *Am. Nat.* 139: 123–147.
- 438 de Roos, A.M. and Persson, L. 2013. *Population and Community Ecology of Ontogenetic*
439 *Development*. – Princeton University Press, Princeton, NJ.
- 440 DeAngelis, D.L. et al. 1993. Fish cohort dynamics: application of complementary modeling
441 approaches. – *Am. Nat.* 142: 604–622.
- 442 Easterling, M.R. et al. 2000. Size-specific sensitivity: applying a new structured population
443 model. – *Ecology* 81: 694–708.
- 444 Ebenman, B. and Persson, L. 1988. *Size-Structured Populations*. – Springer Verlag, Berlin.
- 445 Einum, S. and Fleming, I.A. 2002. Does within-population variation in fish egg size reflect
446 maternal influences on optimal values? – *Am. Nat.* 160: 756–765.
- 447 Ellner, S. and Rees, M. 2006. Integral projection models for species with complex demography. –
448 *Am Nat.* 167: 410–428.

- 449 Ellner, S.P. et al. 2016. Data-driven Modelling of Structured Populations. Springer Switzerland.
- 450 Fox, L. 1975. Cannibalism in natural populations. – *Annu. Rev. Ecol. Evol. Syst.* 6: 87–106.
- 451 Frost, W. and Kipling, C. 1967. A study of reproduction, early life, weight-length relationship
452 and growth of pike, *Esox lucius* L., in Windermere. – *J. Anim. Ecol.* 36: 651–693.
- 453 Hart, S.P. et al. 2016. How variation between individuals affects species coexistence. – *Ecol.*
454 *Lett.* 19: 825–838.
- 455 Hastings, A. and Costantino, R.F. 1991. Oscillations in population numbers - age-dependent
456 cannibalism. – *J. Anim. Ecol.* 60: 471–482.
- 457 Haugen, T. et al. 2007. Density dependence and density independence in the demography and
458 dispersal of pike over four decades. – *Ecol. Monogr.* 77: 483–502.
- 459 Holling, C.S. 1959. Some characteristics of simple types of predation and parasitism. – *Can.*
460 *Entomol.* 91: 395-398.
- 461 Huss, M. et al. 2007. The origin and development of individual size variation in early pelagic
462 stages of fish. – *Oecologia* 153: 57–67.
- 463 Huss, M. et al. 2008. Resource heterogeneity, diet shifts and intra-cohort competition: effects on
464 size divergence in YOY fish. – *Oecologia* 158: 249–257.
- 465 Huss, M. et al. 2010. Intra-cohort cannibalism and size bimodality: a balance between hatching
466 synchrony and resource feedbacks. – *Oikos* 119: 2000–2011.
- 467 Hutchings, J.A. 1997. Life history responses to environmental variability in early life. – In: R.C.
468 Chambers and E.A. Trippel (eds) *Early Life History and Recruitment in Fish Populations*,
469 Chapman and Hall, London, pp. 139–168.
- 470 Johnston, T.A. and Leggett, W.C. 2002. Maternal and environmental gradients in the egg size of
471 an iteroparous fish. – *Ecology* 83: 1777–1791.

- 472 Keast, A. and Eadie, J. 1984. Growth in the first summer of life: a comparison of nine co-
473 occurring fish species. – *Can. J. Zool.* 62: 1242–1250.
- 474 Le Cren, E.D. 2001. The Windermere perch and pike project: a historical review. – *Freshw.*
475 *Forum* 15: 3–34.
- 476 Łomnicki, A. 1988. *Population Ecology of Individuals*. – Princeton University Press, Princeton.
- 477 Marshall, D.J. et al. 2008. Offspring size variation within broods as a bet-hedging strategy in
478 unpredictable environments. – *Ecology* 89: 2506–2517.
- 479 Mittelbach, G.G. and Persson, L. 1998. The ontogeny of piscivory and its ecological
480 consequences. – *Can. J. Fish. Aquat. Sci.* 55: 1454–1465.
- 481 Moran, E.V. et al. 2015. Intraspecific trait variation across scales: implications for understanding
482 global change responses. – *Glob. Change. Biol.* 22: 137–150.
- 483 Nordwall, F. et al. 2001. Intercohort competition effects on survival, movement, and growth of
484 brown trout (*Salmo trutta*) in Swedish streams. – *Can. J. Fish. Aquat. Sci.* 58: 2298–2308.
- 485 Ohlberger, J. et al. 2013. Biotic and abiotic effects on cohort size distributions in fish. – *Oikos*
486 122: 835–844.
- 487 Olsen, E.M. et al. 2009. Nine decades of decreasing phenotypic variability in Atlantic cod. –
488 *Ecol. Lett.* 12: 622–631.
- 489 Peacor, S.D. et al. 2007. Mechanisms of nonlethal predator effect on cohort size variation:
490 Ecological and evolutionary implications. – *Ecology* 88: 1536–1547.
- 491 Pereira, L.S. et al. 2017. Is there a relationship between fish cannibalism and latitude or species
492 richness? – *PLoS ONE* 12: e0169813–14.
- 493 Persson, L. et al. 2006. Temporal stability in size distributions and growth rates of three *Esox*
494 *lucius* L. populations. A result of cannibalism? – *J. Fish Biol.* 69: 461–472.

- 495 Persson, L. et al. 2003. Gigantic cannibals driving a whole-lake trophic cascade. – Proc. Natl.
496 Acad. Sci. USA 100: 4035-4039.
- 497 Persson, L. et al. 2004. Cannibalism in a size-structured population: Energy extraction and
498 control. – Ecol. Monogr. 74: 135–157.
- 499 Pfister, C. and Stevens, F. 2002. The genesis of size variability in plants and animals. – Ecology
500 83: 59–72.
- 501 Philippi, T. and Seger, J. 1989. Hedging one's evolutionary bets, revisited. – Trends Ecol. Evol.
502 4: 41–44.
- 503 Polis, G. 1981. The evolution and dynamics of intraspecific predation. – Annu. Rev. Ecol. Evol.
504 Syst. 12: 225–251.
- 505 R Core Team 2016. R: A language and environment for statistical computing. – R Foundation for
506 Statistical Computing, Vienna, Austria. URL <https://www.R-project.org>
- 507 Rasmussen, N.L. and Rudolf, V.H.W. 2015. Phenological synchronization drives demographic
508 rates of populations. – Ecology 96: 1754–1760.
- 509 Rudolf, V.H.W. 2007. The interaction of cannibalism and omnivory: consequences for
510 community dynamics. – Ecology 88: 2697–2705.
- 511 Simmonds, E.G. and Coulson, T. 2014. Analysis of phenotypic change in relation to climatic
512 drivers in a population of Soay sheep *Ovis aries*. – Oikos 124: 543–552.
- 513 Thackeray, S.J. et al. 2013. Food web de-synchronisation in England's largest lake: an assessment
514 based upon multiple phenological metrics. – Glob. Change Biol. 19: 3568–3580.
- 515 Uchmanski, J. 1985. Differentiation and frequency-distributions of body weights in plants and
516 animals. – Phil. Trans. R. Soc. B 310: 1-75.

- 517 van Densen, W. et al. 1996. Intra-cohort variation in the individual size of juvenile pikeperch,
518 *Stizostedion lucioperca*, and perch, *Perca fluviatilis*, in relation to the size spectrum of their
519 food items. – *Ann. Zool. Fenn.* 33: 495–506.
- 520 van Kooten, T. et al. 2004. Local foraging and limited mobility: Dynamics of a size-structured
521 consumer population. – *Ecology* 85: 1979–1991.
- 522 van Kooten, T., et al. 2010. Size at hatching determines population dynamics and response to
523 harvesting in cannibalistic fish. – *Can. J. Fish. Aquat. Sci.* 67: 401–416.
- 524 Vindenes, Y. and Langangen, Ø. 2015. Individual heterogeneity in life histories and eco-
525 evolutionary dynamics. – *Ecol. Lett.* 18: 417–432.
- 526 Vindenes, Y. et al. 2014. Effects of climate change on trait-based dynamics of a top predator in
527 freshwater ecosystems. – *Am. Nat.* 183: 243–256.
- 528 Vindenes, Y. et al. 2016. Fitness consequences of early life conditions and maternal size effects
529 in a freshwater top predator. – *J. Anim. Ecol.* 85: 692–704.
- 530 Winfield, I.J. et al. 2012. Long-term changes in the diet of pike (*Esox lucius*), the top aquatic
531 predator in a changing Windermere. – *Freshw. Biol.* 57: 373–383.
- 532 Winfield, I.J. et al. 2013a. Pike growth data 1944–1995. – NERC Environmental Information
533 Data Centre, [http://dx. doi.org/10.5285/637d60d6-1571-49af-93f7-24c1279d884d](http://dx.doi.org/10.5285/637d60d6-1571-49af-93f7-24c1279d884d).
- 534 Winfield, I.J. et al. 2013b. Pike survival data 1953–1990. – NERC Environmental Information
535 Data Centre, [http://dx. doi.org/10.5285/813e07dd-2135-49bc-93c6-83999e442b36](http://dx.doi.org/10.5285/813e07dd-2135-49bc-93c6-83999e442b36).
- 536 Winfield, I.J. et al. 2015. Windermere pike fecundity and egg data 1963–2003. – NERC
537 Environmental Information Data Centre, [http://dx.doi.org/10.5285/4b255fc4-33d3-4beb-](http://dx.doi.org/10.5285/4b255fc4-33d3-4beb-a238-37e1a8cf32a2)
538 [a238- 37e1a8cf32a2](http://dx.doi.org/10.5285/4b255fc4-33d3-4beb-a238-37e1a8cf32a2).

539 Wright, P.J. and Trippel, E.A. 2009. Fishery-induced demographic changes in the timing of
540 spawning: consequences for reproductive success. – *Fish Fish.* 10: 283–304.

For Review Only

541 **Table 1: Overview of variables in the IPM**

542

Variable	Explanation
x, y	State variable of size at time of census, for victims and cannibals
x'	Next year's size (before census) or offspring size
t	Time
$\mathbf{n}_t = n_t(x)$	Population size distribution at time t
$n_t^*(x')$	Population size distribution after growth and survival
$R_t(x')$	Offspring population size distribution after first density regulation
$O_t(x')$	Offspring distribution after intercohort cannibalism at age 1
$m(x)$	Fecundity (average egg number)
$p_m(x)$	Probability of maturity
$s_t(x)$	Survival probability from t to $t + 1$, depending on $n_t(x)$.
$s_t^*(x)$	Survival probability from t to $t + 1$, depending on $n_t^*(x)$.
$g(x'; x)$	Growth distribution (lognormal)
• $\mu_g(x)$	Mean of x' after growth (non-offspring), following a von Bertalanffy model.
• $\sigma_g^2(x)$	Conditional variance of x' after growth, given current size x .
$f_t(x')$	Offspring length distribution (lognormal) at age 1, depending on total egg number M_t
• $\mu_{L1,t}$	Mean of x' in offspring, depending on total egg number M_t
• σ_{L1}^2	Variance in offspring size at age 1

543 **Table 2: Overview of model parameters and baseline values.**

Process	Parameter	Description	Value	Units
Background survival	α_{sb}	Size at maximum survival	80	mm
	s_{b0}	Maximum survival	0.85	-
	β_{sb}	Decline in survival at smaller and larger sizes	-0.0005	mm^{-2}
Cannibalism survival	μ_{cn}	Location parameter	-1.5	$mm\ mm^{-1}$
	σ_{cn}	Scale parameter	0.3	$mm\ mm^{-1}$
	β_{cn}	Cannibalism intensity	0.01	$mm^{-\alpha_{cn}}$
	α_{cn}	Intensity size exponent	0.6	-
	δ_{cn}	Type of functional response	0.1	-
von Bertalanffy growth function	L_{∞}	Asymptotic average length	109	mm
	K	Growth rate coefficient	0.21	-
Variance in growth	ν_g	Growth variance exponent	-0.015	-
	τ_g	Growth variance scalar	5	-
Maturation	μ_p	Size at 50% maturation probability	41.5	mm
	σ_p	Width of maturation probability function	0.5	-
Fecundity	α_m	Fecundity constant	0.095	$ind\ mm^{-\beta_m}$
	β_m	Fecundity exponent	3.3	-
Offspring density	α_R	Maximum per capita recruitment	4e-4	$ind\ ind^{-1}$
	β_R	Determines carrying capacity	1e-8	ind
Offspring size distribution	β_{OL1}	Constant of mean offspring size depending on egg density	3.85	$\ln(mm)$
	β_{ML1}	Exponent of mean offspring size depending on egg density	0.04	$\ln(mm)$

544 ind = individuals

545 **FIGURE CAPTIONS**

546 **Figure 1: Timing of annual life-history events.** n_t is the population size distribution at time t ,
 547 M_t is the total number of eggs produced by the population, $R_t = R_t(x)$ is the population
 548 distribution of offspring before intercohort cannibalism occurs, $O_t = O_t(x)$ is the population
 549 distribution of age-1 offspring entering the next census, and $n_t^* = n_t^*(x)$ is the population
 550 distribution after density dependent survival and growth have occurred. The green colour
 551 indicates size-independent density regulation among offspring, while the blue indicates size-
 552 dependent cannibalism affecting the survival of both offspring and older individuals. Solid
 553 arrows indicate the sequence of annual events and the dashed arrow indicates an interaction.

554 **Figure 2: Basic model functions.** (a) Size-dependent cannibalism kernel for different cannibal
 555 sizes, (b) background survival probability with no cannibalism, (c) mean length next year (black)
 556 and zero growth line (grey) (d) number of offspring (age 1) as a function of egg number, (e)
 557 probability of maturity (dashed line) and fecundity (solid line) as a function of size, and (f) the
 558 offspring size distribution (at age 1) for different values of size variance. Back-calculated length
 559 data (c) and fecundity data (e) for Windermere pike are also shown (filled circles).

560 **Figure 3: Bifurcation diagram.** Shown is the population size as a function of the variance in
 561 offspring length (σ_{L1}^2). Projections were run for 1000 time steps, and population size was
 562 sampled for the last 100 time steps.

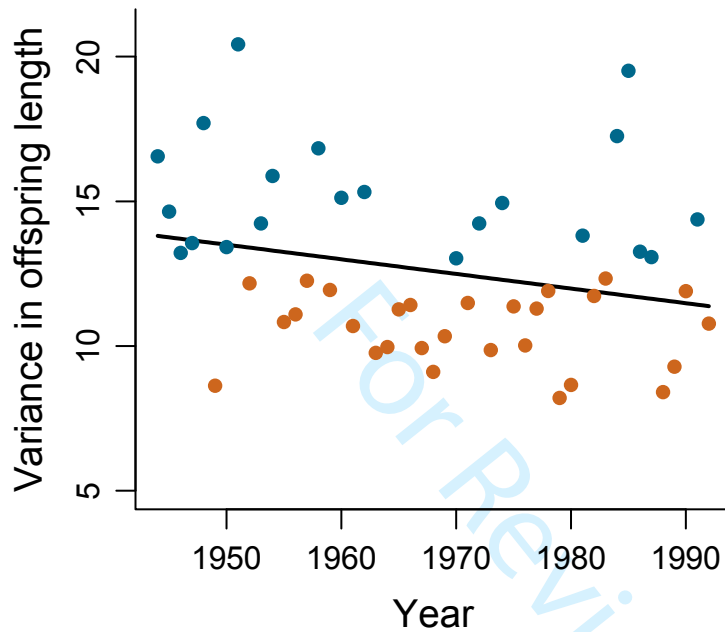
563 **Figure 4: Unstable and stable dynamics.** Shown are population densities over time (a, b), size
 564 distributions (c, d), and annual probabilities of surviving cannibalism as a function of victim size
 565 (e, f) for two values of offspring size variance representing unstable (left, $\sigma_{L1}^2 = 3$) and stable
 566 dynamics (right, $\sigma_{L1}^2 = 10$). Projections were run for 1000 time steps, and size distributions and

567 survival curves were plotted for the last 10 time steps to illustrate the unstable dynamics at low
568 offspring size variance.

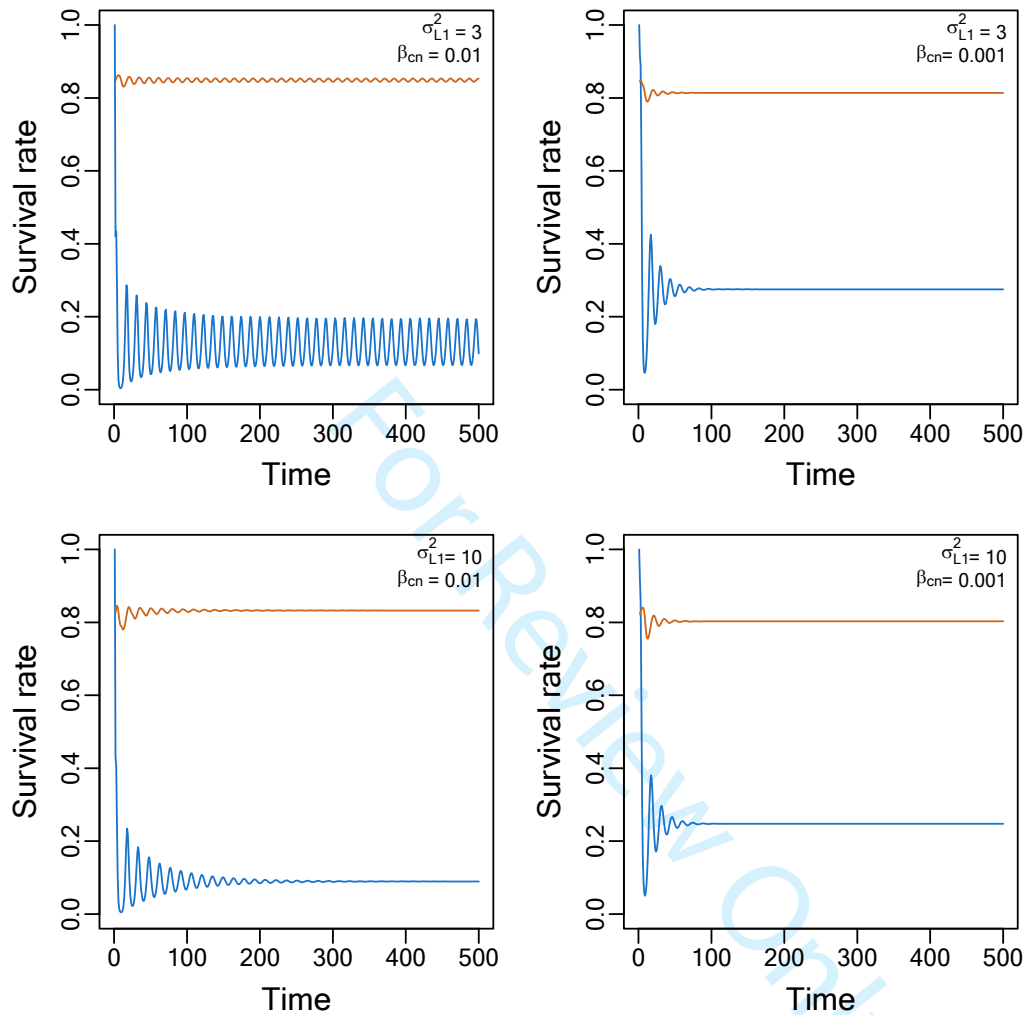
For Review Only

1 SUPPLEMENTARY MATERIAL

2 Appendix 1: Data figure



3
4 **Figure A1: Size variance in pike.** Time series of the variance in body length (cm²) for offspring
5 (age-1) pike from Windermere, UK, suggesting a negative trend over time (slope=-0.05; p-
6 value=0.08). Data were based on back-calculated lengths from individuals captured at age 3 and
7 older. Colours indicate values above (blue, dark) and below (orange, light) the long-term average.

8 **Appendix 2: Offspring survival**

9

10 **Figure A2: Cannibalism and background survival of offspring.** Shown are offspring survival
 11 rates resulting from intercohort cannibalism (blue) and background mortality (orange) for low
 12 offspring size variance (top, $\sigma_{L1}^2 = 3$) and high offspring size variance (bottom, $\sigma_{L1}^2 = 10$) and
 13 moderate (left, $\beta_{cn} = 0.01$) and low (right, $\beta_{cn} = 0.001$) cannibalism intensity (500 time steps,
 14 all other parameters as in baseline model). Survival rates do not stabilize over time in case of low
 15 size variance and moderate cannibalism (top left) thus leading to unstable population dynamics.

16 **Appendix 3: Incorporating competition into the model**

17 Here we describe the methods and results for an extended version of our model that includes size-
 18 dependent intraspecific competition in addition to cannibalism. Size-dependent competition can
 19 be modelled in a number of different ways, although considering all possible effects of
 20 competition is beyond the scope of this study. We consider a scenario where size-dependent
 21 competition affects growth and survival and investigate how the main result (that offspring size
 22 variation promotes population stability) is affected.

23 In this model, competition is assumed to affect somatic growth and survival. Competitive
 24 interactions are governed by a competition kernel $C_{cp}(x,y)$, which describes the potential
 25 interaction strength between an individual of size x and a competitor of size y (
 26 $\int_0^\infty C_{cp}(x,y)dx = 1$). We assume that competition is most fierce between individuals of the same
 27 size, e.g. because they have similar diet or habitat preferences. Specifically, the competition
 28 intensity experienced by an individual of size x due to potential competitors of size y is given by
 29 a lognormal distribution with scale parameter σ_{cp} and location parameter $\log(x) + \sigma_{cp}^2$. The
 30 competition kernel describes the potential effect of an individual of a given size on other
 31 individuals across the size range through competitive interactions (Figure A3). Asymmetric
 32 competition for shared resources, for instance when juveniles and adults compete for the same
 33 prey species in the same habitat, is not reflected by this competition kernel.

34 Here, survival probability depends on background survival, competition, and cannibalism: $s_t(x)$
 35 $= s_b(x) s_{cn,t}(x) s_{cp,t}(x)$. The probability of surviving competition is given by $s_{cp,t}(x) = \exp$
 36 $\left(- \int_0^\infty \beta_{cpS} y^{\alpha_{cpS}} C_{cp}(x,y) n_t(y) dy \right)$, where β_{cpS} determines the effect size of competition on
 37 survival (higher β_{cpS} values imply stronger effects on survival), while α_{cpS} scales the competitive

38 intensity over competitor length y . Growth is also depending on competition in this model,
 39 through the mean length next year, given current length x and population density $n_t(x)$. This is
 40 given by $\mu_{g,t}(x) = \ln [KL_\infty + (1 - K)x] - g_{cp,t}(x)$, where the last term describes the effect of
 41 competition and is scaled by the effect size β_{cpG} : $g_{cp,t}(x) = \beta_{cpG} x^{\alpha_{cpG}} \int_0^\infty n_t(x_{cp}) C_{cp}(x_{cp};x) dx_{cp}$.
 42 The term α_{cpG} determines how the competitive intensity changes over length x , and integration is
 43 over competitor lengths x_{cp} .

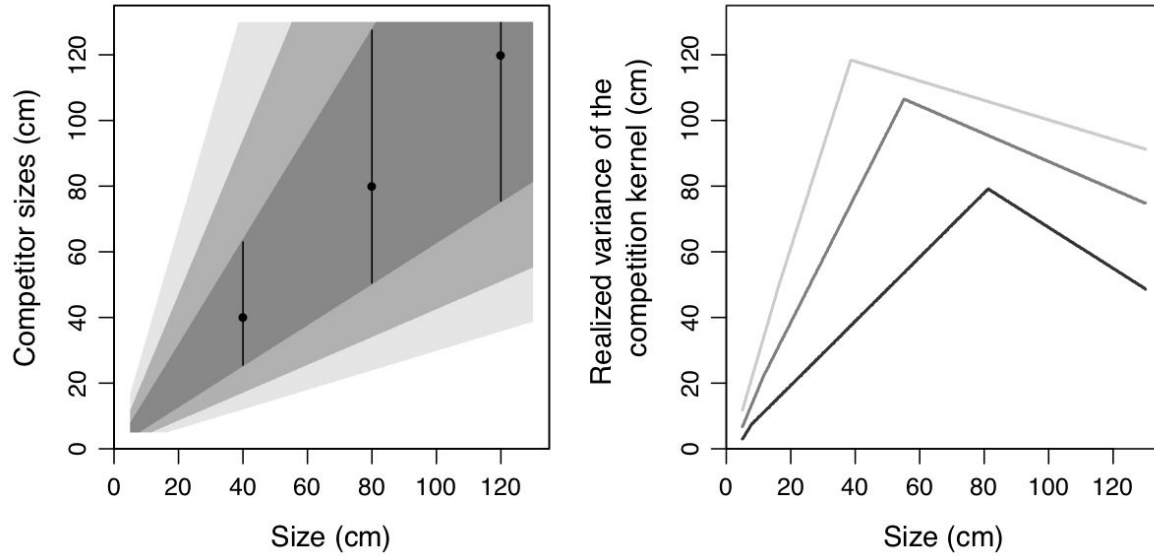
44 ***Parameterization***

45 The effect of competition on growth could not be estimated from the data and was thus varied in
 46 the model analysis. The default parameter was set to $\beta_{cpG} = 1 \cdot 10^{-5}$ (scaling parameter $\alpha_{cpG} = 1$) to
 47 achieve reasonable effects of competition on the mean growth rate (i.e. biologically realistic
 48 ranges). Here, von Bertalanffy parameters were set to $K = 0.2$ and $L_\infty = 120$, so that growth
 49 patterns correspond to empirical patterns under intermediate population densities. The
 50 competition effect on survival was assumed to be an order of magnitude smaller than the effect of
 51 competition on growth ($\beta_{cpS} = 0.1 \beta_{cpG}$, and scaling parameter $\alpha_{cpS} = 0$).

52 ***Results***

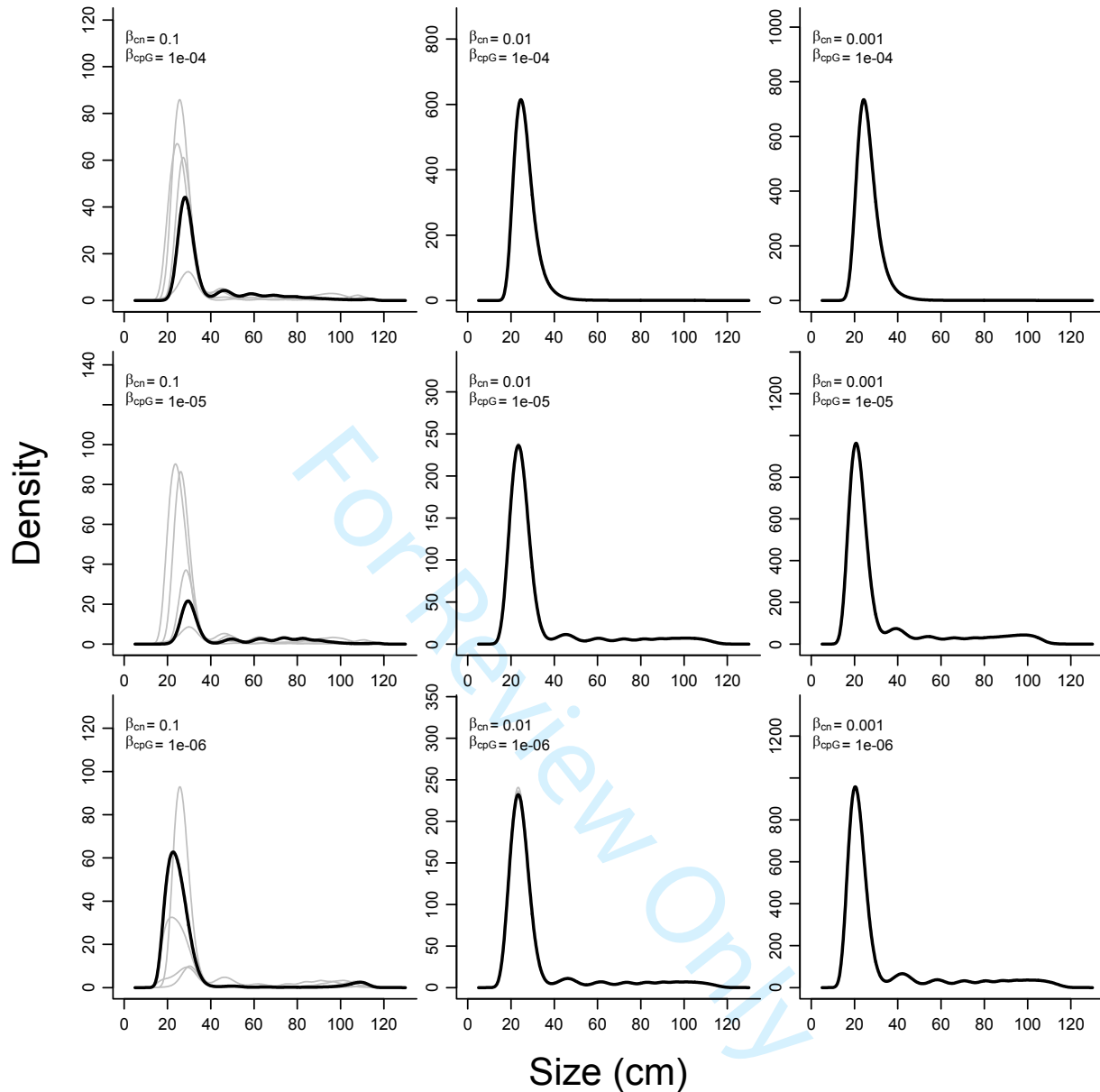
53 The shape of the population size distribution and the stability of the population dynamics also
 54 depend on the strength of competition, in addition to the strength of cannibalism. Increased
 55 competition causes a smoother size distribution with less distinct peaks for older cohorts, whereas
 56 cannibalism causes more pronounced peaks in the size distribution due to a reduction in density
 57 and thus competition (Figure A4). Ultimately, very strong competition causes somatic growth to
 58 approach zero, which results in a unimodal size distribution. **Previous work has shown that**
 59 **competition can lead to size convergence within cohorts due to exploitative interactions when**

60 small individuals are competitively superior, or increased size variation, for instance when
61 alternative prey resources are available or social dominance structures allow for resource
62 monopolization (Huss et al. 2007, 2008, 2010). The strengths of the intraspecific interactions thus
63 determine if and where the transition from unstable to stable dynamics occurs (Figure A5). As
64 competition decreases and cannibalism increases, the transition appears and shifts to larger size
65 variances. The degrees of competition and cannibalism were varied widely in order to cover a
66 broad range of ecologically relevant interaction strengths. The lowest and highest values used for
67 the two interactions thus represent large variation in growth rates and survival probabilities
68 (Figure A6). For example, for offspring of 25 cm (approximately the mean length at age-1 in the
69 baseline model), the probability of surviving cannibalism varied between about 0.004 and 0.992,
70 while the mean annual growth rate varied between 0% and 76% across all combinations of
71 cannibalism and competition intensities considered in the analysis.



72

73 **Figure A3:** Illustration of the competition kernel. The left plot shows the size range of
 74 competitors as a function of the size of the focal individual (for different quantiles of the
 75 competition kernel, shaded grey areas). For three focal sizes (40, 80, 120 cm), the range (black
 76 lines) and mode (circles) of the kernel are highlighted. The right plot shows the realized variance
 77 of the competition kernel for all focal sizes (taking into account the lower and upper size limits)
 78 to illustrate that the width of the competition window reaches a maximum at intermediate sizes.



79

80 **Figure A4: Stable size distribution for different degrees of competition and cannibalism.**

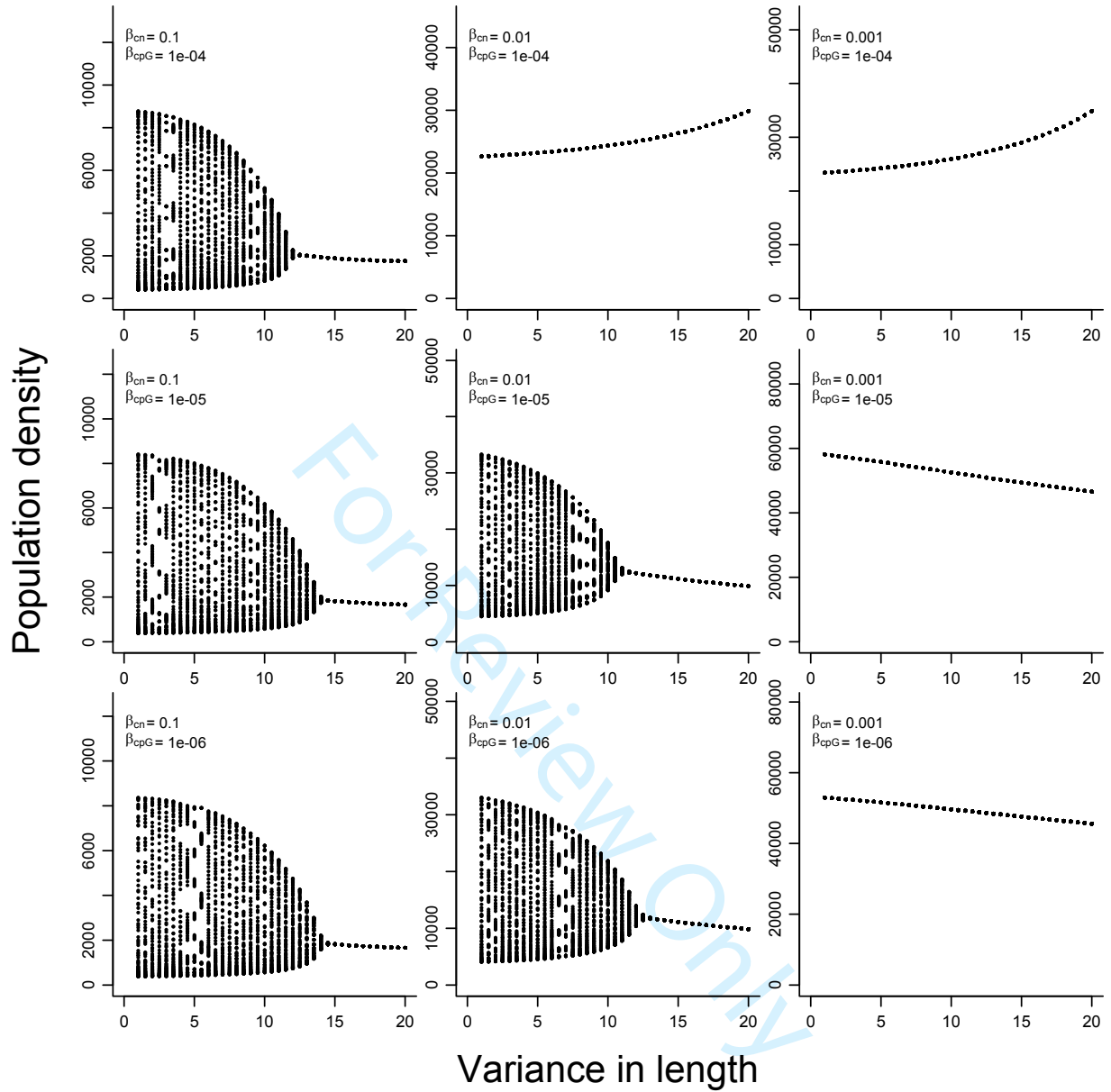
81 Thick black lines indicate the size distribution after the maximum number of time steps ($t=1000$).

82 Thin grey lines indicate the size distribution 1, 3, 5, and 10 years earlier to indicate whether the

83 dynamics are stable or unstable. The default value of 13 was used for the offspring size variance.

84 Cannibalism intensity decreases from left ($\beta_{cn} = 0.1$) to right ($\beta_{cn} = 0.001$), and competition

85 intensity increases from bottom ($\beta_{cpG} = 1e^{-6}$) to top ($\beta_{cpG} = 1e^{-4}$).



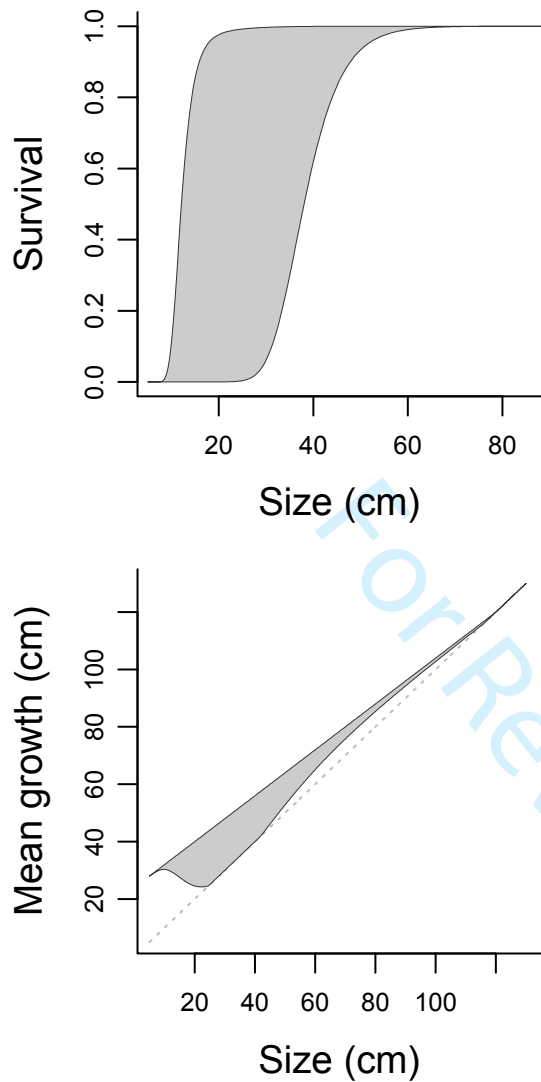
86

87 **Figure A5:** Bifurcation diagrams of population density against the variance in offspring length.

88 Projections were run for 1000 time steps and population density was sampled for the last 100

89 time steps. Cannibalism intensity decreases from left ($\beta_{cn} = 0.1$) to right ($\beta_{cn} = 0.001$), and90 competition intensity increases from bottom ($\beta_{cpG} = 1e^{-6}$) to top ($\beta_{cpG} = 1e^{-4}$). These values

91 were chosen to represent a broad range of survival probabilities and mean growth rates.

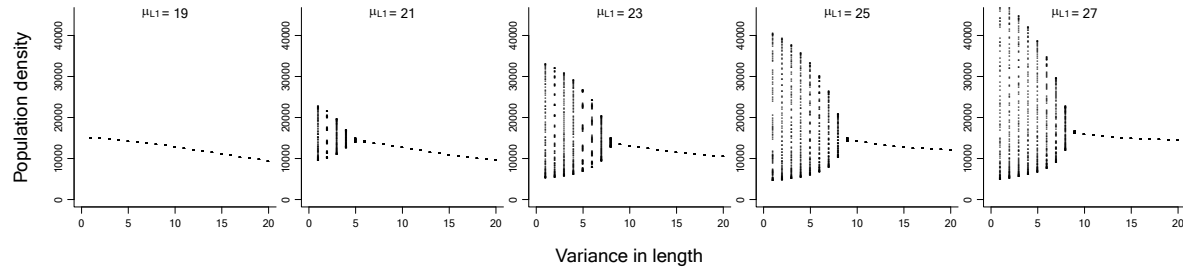


92

93 **Figure A6:** Cannibalism survival probabilities and mean growth rates for the range of
 94 cannibalism and competition intensities considered in the additional model analyses. The dotted
 95 line represents zero growth. The plot was produced by setting σ_{L1}^2 to 16 instead of the default
 96 value, which resulted in stable dynamics for all tested combinations of cannibalism and
 97 competition intensities.

98 **Appendix 4: Additional sensitivity tests**

99 The following sensitivity analyses were performed to further scrutinize further our results
100 with respect to important parameters in the model. First, a bifurcation analysis for
101 different mean values of the offspring size distribution showed that the shift to unstable
102 dynamics at low size variance occurred for a large range of mean sizes of about 21-27
103 cm, but that this pattern disappeared at smaller mean sizes (Figure A7). This suggests
104 that a transition to unstable dynamics at low size variance is expected for the range of
105 mean offspring sizes observed in Windermere pike (~21-26 cm). Second, in addition to
106 cannibalism intensity, the relative victim-to-cannibal size ratio and the width of the
107 cannibalism kernel affect the size distribution and population stability. Population
108 dynamics stabilize at a higher mean victim-to-cannibal size ratio (Figure A8), and a wider
109 cannibalism kernel (Figure A9), because a wide diet range of cannibals contributes to a
110 smoother size distribution through spreading the predation risk across the victim size
111 range. **Finally, we show that and the stability-instability transition occurs at lower**
112 **variance values when individual growth variation is increased (Figure A10).**



113

114 **Figure A7: Bifurcation diagrams of population density over variance in offspring**

115 **size for different values of mean offspring size.** In order to investigate whether the

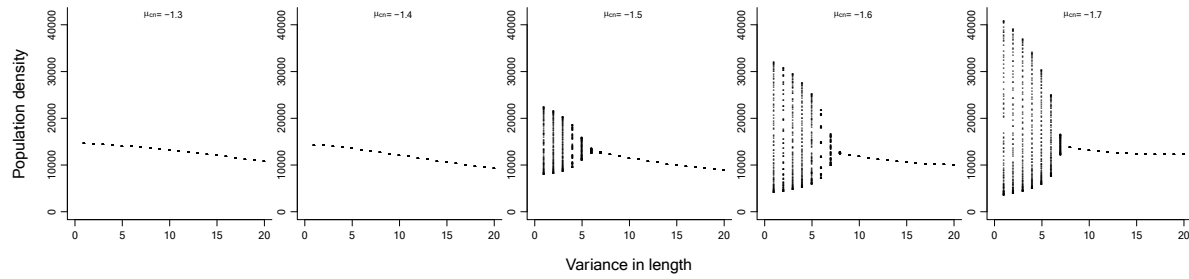
116 shift to unstable dynamics at low size variance would occur at different values of mean

117 offspring size (default value at ~ 23 cm), we fixed the mean offspring size such that it

118 would not depend on total egg number. The range of mean offspring sizes observed in

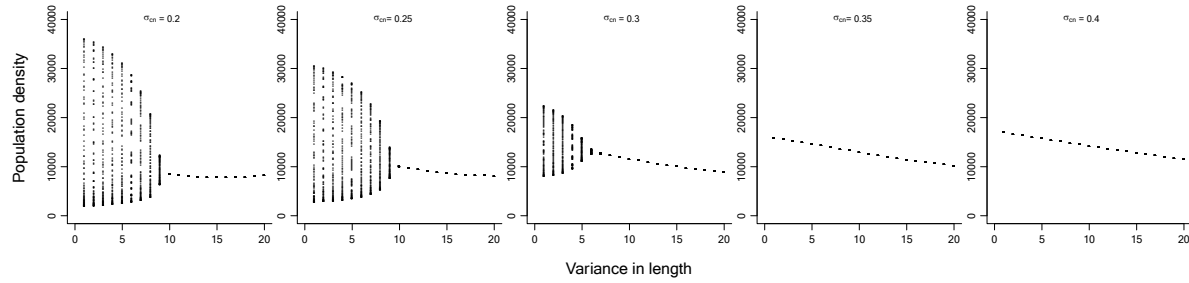
119 Windermere pike across years is about 21-26 cm, and the range shown here is 19 cm

120 (left) to 27 cm (right).



121

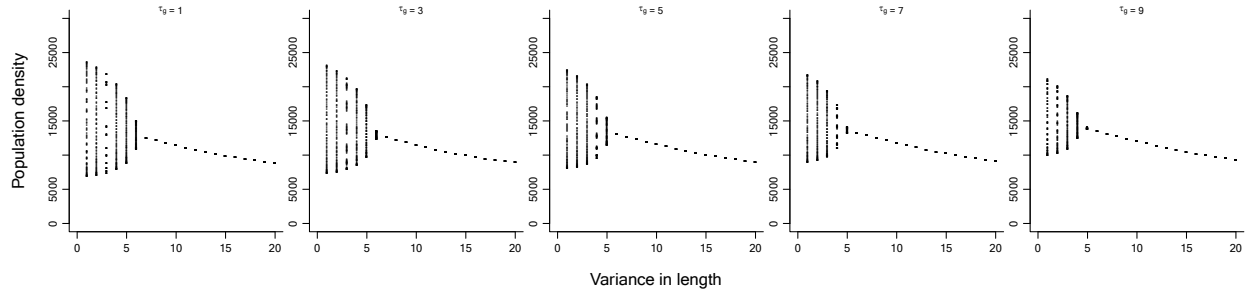
122 **Figure A8:** Bifurcation diagrams of population density against variance in offspring
 123 length for different values of the mean victim-to-cannibal size ratio (μ_{cn}). Values of μ_{cn}
 124 range from -1.3 (left) to -1.7 (right). The location parameter μ_{cn} is defined on the log
 125 scale.



126

127 **Figure A9:** Bifurcation diagrams of population density against variance in offspring
 128 length for different values of the standard deviation in the victim-to-cannibal size ratio.
 129 Values of σ_{cn} range from 0.2 (left) to 0.4 (right).

130



131

132 **Figure A10:** Bifurcation diagrams of population density against variance in offspring133 length for different values of growth variation (τ_g). Values of τ_g range from 1 (left) to 9

134 (right).

For Review Only

